Atmos. Chem. Phys. Discuss., https://doi.org/10.5194/acp-2017-951
Manuscript under review for journal Atmos. Chem. Phys.
Discussion started: 25 October 2017

Atmospheric Chemistry and Physics Discussions

Effects of tropical deep convection on interannual variability of tropical tropopause layer water vapor

Hao Ye, Andrew E. Dessler, and Wandi Yu

Department of Atmospheric Sciences, Texas A&M University, College Station, USA

Correspondence to: Andrew E. Dessler (adessler@tamu.edu)

Abstract. Water vapor interannual variability in the tropical tropopause layer (TTL) is investigated using satellite observations and model simulations. We breakdown the influences of the Brewer-Dobson circulation (BDC), the quasi-biennial oscillation (QBO), and the tropospheric temperature (ΔT) as a function of latitude and longitude using a 2-dimensional multivariable linear regression. This allows us to examine the spatial distribution of the impact on TTL water vapor from these physical processes. In agreement with expectation, we find that the impacts from the BDC and QBO act on TTL water vapor by changing TTL temperature. For ΔT, we find that TTL temperatures alone cannot explain the influence. We hypothesize a moistening role for the evaporation of convective ice from increased deep convection as troposphere warms. Tests with simulations from GEOSCCM and a corresponding trajectory model support this hypothesis.

1 Introduction

Stratospheric water vapor plays an important role in both the chemistry (Stenke and Grewe, 2005) and radiative energy budget (Solomon et al., 2010; Dessler et al., 2013) of the atmosphere. Air enters the stratosphere from the tropical troposphere mainly through the tropical tropopause layer (TTL, ∼15-18 km) (Sherwood and Dessler, 2000; Fueglistaler et al., 2009), which serves as a transition region between the troposphere and stratosphere. It is generally recognized that the coldest temperature in the TTL acts like a "cold trap" that provides primary control on the amount of water vapor entering the lower stratosphere (Mote et al., 1996; Holton and Gettelman, 2001). Large interannual variations of TTL water vapor have been observed and attributed to a set of physical processes that affect water vapor by varying TTL temperatures, such as the quasi-biennial oscillation (QBO) (Geller et al., 2002; Fueglistaler and Haynes, 2005; Dessler et al., 2013) and the Brewer-Dobson circulation (BDC) (Randel et al., 2006; Calvo et al., 2010).

Another important process is the deep convection that reaches the TTL. Such convection can moisten the tropical lower stratosphere by evaporation of injected ice particles (Corti et al., 2008). The efficiency of this process is strongly related to ambient relative humidity (Dessler and Sherwood, 2004; Wright et al., 2009) because high relative humidity inhibits evaporation. Recent aircraft measurements (Anderson et al., 2012; Herman et al., 2017) and satellite observations (Dessler and Sherwood, 2004; Schwartz et al., 2013; Sun and Huang, 2015) confirm that the deep convection enhances lower stratospheric water vapor over the North American summer monsoon region, where relative humidity is very low.

Atmos. Chem. Phys. Discuss., https://doi.org/10.5194/acp-2017-951
Manuscript under review for journal Atmos. Chem. Phys.
Discussion started: 25 October 2017

Atmospheric Chemistry and Physics Discussions

In the tropics, the influence of convection on observed water vapor amounts is less clear. It seems certain that convective ice evaporation at least occasionally moistens the stratosphere (Khaykin et al., 2009; Hassim and Lane, 2010; Carminati et al., 2014; Schoeberl et al., 2014; Frey et al., 2015; Ueyama et al., 2015; Virts and Houze Jr, 2015), but the impact of convection there is muted because the relative humidity of the TTL is high, suppressing evaporation, and only convection reaching above the cold point will significantly impact the stratosphere (Dessler et al., 2007). This makes identifying convective impacts difficult, although a recent analysis has shown that evaporation of convective ice could account for a significant part of the TTL water vapor response to the strong El Niño of 2015-2016 (Avery et al., 2017).

On longer time scales, though, the impact of ice evaporation on stratospheric water vapor could be much more important. Almost all climate models predict that the water vapor in the UTLS will increase over the next century (Gettelman et al., 2010), and a significant fraction of this increase is due to the evaporation of lofted ice from deep convection (Dessler et al., 2016). This gives us ample motivation to look more closely at the impact of convective ice evaporation on TTL water vapor in the observations.

The purpose of this study is to investigate in more detail the physical processes controlling the interannual variations of water vapor in the TTL. Previous work (Dessler et al., 2013, 2014) has shown that the QBO, the strength of the BDC, and the tropical tropospheric temperature can explain most of the variance in the interannual variations in *tropical average* TTL water vapor. In this paper, we extend this previous work by investigating whether these variables can also explain the spatial distribution of the interannual variability.

2 Data and Methods

2.1 MLS water vapor

The observations of TTL water vapor used are from the Earth Observing System (EOS) Aura Microwave Limb Sounder (MLS) (Lambert et al., 2007; Read et al., 2007). The MLS instrument has obtained continuous high quality global observations of water vapor in the upper troposphere and stratosphere since August 2004. The data is available from https://mls.jpl.nasa.gov/. Here we use MLS version 4.2 level 2 water vapor retrievals from August 2004 to December 2016. The daily water vapor mixing ratio measurements are binned and averaged to produce monthly data on a $4^\circ \times 8^\circ$ latitude and longitude grid with the quality control following the instruction in Livesey et al. (2017). We focus on the interannual anomalies of water vapor from 30°N to 30°S at 100 hPa. The interannual anomaly of water vapor at each grid point is calculated by subtracting the average annual cycle at this grid point.

2.2 GEOSCCM

We also use simulations of TTL water vapor from the Goddard Earth Observing System Chemistry Climate Model (GEOSCCM) in this study. The state-of-the-art GEOSCCM includes the GEOS-5 atmospheric general circulation model (Molod et al., 2012) with detailed cloud microphysical schemes (Barahona et al., 2014) and the "Combo CTM" tropospheric/stratospheric chemical

Atmos. Chem. Phys. Discuss., https://doi.org/10.5194/acp-2017-951
Manuscript under review for journal Atmos. Chem. Phys.
Discussion started: 25 October 2017

Atmospheric Chemistry and Physics Discussions

package (Duncan et al., 2007). The GEOSCCM simulation provides long term simulations of temperature, water vapor, horizontal winds, diabatic heating rates, and convective ice with a resolution of 2°× 2.5° in latitude and longitude on 72 vertical model levels, up to 0.01 hPa. In this study, we investigate the water vapor simulation from GEOSCCM in the TTL during the MLS period. As these simulations are from a free-running GEOSCCM, it can only be used for statistical analysis and is not directly comparable to observed water vapor variations.

2.3 Trajectory model

We also produce simulations of TTL water vapor using a domain-filling forward trajectory model, which accurately reproduces water vapor, ozone, and carbon monoxide anomalies in the TTL and lower stratosphere (Schoeberl and Dessler, 2011; Schoeberl et al., 2012, 2013; Dessler et al., 2014; Wang et al., 2014).

This model uses Bowman's trajectory code (Bowman, 1993; Bowman and Carrie, 2002). The parcels are driven by horizontal winds and total diabatic heating rates from reanalysis datasets and from the GEOSCCM. When comparing to MLS data, we use trajectory runs driven by two reanalysis datasets: the European Centre for Medium-Range Weather Forecasts (ECMWF) ERA-interim reanalysis (ERAi) (Dee et al., 2011) and the NASA's Modern-Era Retrospective-Analysis for Research and Applications Version-2 (MERRA-2) (Bosilovich et al., 2016). When comparing to GEOSCCM output, we drive the model with meteorological fields from the GEOSCCM.

In all simulations, 1350 parcels are initialized every day from January 2000 to December 2016 on an equal area grid from 60°N to 60°S. The parcels are released on the 370-K isentropic level, which is just above the zero net diabatic heating level over the tropics (∼355-360 K) but below the cold point (∼375-380 K). Each parcel travels forward following the horizontal winds and diabatic heating rate. Once a parcel has a pressure larger than 250 hPa, it is regarded as having descended back into the troposphere and is removed from the model.

Each parcel is initialized with a water vapor mixing ratio of 200 parts per million by volume (ppmv). Along the trajectory, a parcel will immediately be dehydrated to saturation once its water vapor mixing ratio exceeds a predetermined saturation threshold, 100% in this study. The saturated water vapor mixing ratio is obtained from the thermodynamic equation with respect to ice (Murphy and Koop, 2005) based on temperatures from reanalyses or the GEOSCCM. The production of water vapor from methane oxidation is also included in these trajectory model runs but it has very little effect on water vapor in the TTL (Dessler et al., 2014).

The water vapor mixing ratio from the trajectory model is gridded into 4°× 8° bins, just as the MLS data were. In the vertical, the trajectory output is binned by averaging the parcels in a pressure range around each MLS or GEOSCCM level. In comparisons to MLS, the gridded water vapor mixing ratio is then re-averaged using the MLS averaging kernels following the instruction from Livesey et al. (2017). When doing this kernel averaging, grid boxes with no trajectory parcels (mostly at low altitudes) are filled with monthly water vapor mixing ratios from the reanalyses (ERAi and MERRA-2). Sensitivity tests confirm that changing water vapor mixing ratio from the reananlyses has no impact on the spatial distribution of the interannual variability of TTL water vapor that is the focus of this paper.

Atmos. Chem. Phys. Discuss., https://doi.org/10.5194/acp-2017-951
Manuscript under review for journal Atmos. Chem. Phys.
Discussion started: 25 October 2017

Atmospheric Chemistry and Physics Discussions

2.4 Convection

We also use estimates of convective occurrence produced by combining geostationary infrared satellite imagery and rainfall measurements (Pfister et al., 2001; Bergman et al., 2012; Ueyama et al., 2015). The data have a horizontal resolution of $0.25° \times 0.25°$ and a temporal resolution of 3 hours and cover the period from 2005 to 2016. In this paper, we use the cloud-top height and cloud-top potential temperature to estimate the convective cloud occurrence frequency in the TTL, which we take to be an indicator of the convective influence on the TTL. These data are available from https://bocachica.arc.nasa.gov/~lpfister/cloudtop/.

3 Results

3.1 Influence of the BDC and QBO on TTL water vapor

Fig. 1 shows the monthly and tropical averaged 100-hPa H_2O anomalies from MLS observations and from trajectory model runs driven by meteorology from ERAi (traj_ERAi) and MERRA-2 (traj_MERRA2). Similar to the results in Dessler et al. (2013, 2014) at 82 hPa, there is a good agreement between the observations and trajectory models at 100 hPa.

Dessler et al. (2013, 2014) also showed that we can fit tropical average values of 82-hPa H_2O anomalies with a simple linear model:

$$\mathrm{H_2O} = a \cdot \mathrm{BDC} + b \cdot \mathrm{QBO} + c \cdot \Delta T + r, \tag{1}$$

where BDC, QBO, and ΔT are indices representing the strength of the Brewer-Dobson circulation, the phase of the QBO, and the tropospheric temperature anomalies of the tropical climate system, respectively. We can also fit the 100 hPa H_2O with the same model based on the regressors from ERAi and MERRA-2, with R^2 of 0.78 and 0.58, respectively.

To help us gain additional physical insight into that result, in this paper we perform a similar multivariable regression, but at individual grid points in the TTL:

$$\mathrm{H_2O}(x_i, y_j) = a(x_i, y_j) \cdot \mathrm{BDC} + b(x_i, y_j) \cdot \mathrm{QBO} + c(x_i, y_j) \cdot \Delta T + r(x_i, y_j). \tag{2}$$

Here, $\mathrm{H_2O}(x_i, y_j)$ represents the H_2O anomaly time series at 100 hPa in a grid-box centered at longitude x_i and latitude y_j. The coefficients a, b, and c, as well as the residual term r, are also functions of latitude and longitude.

The regressors in Eq. 2 are the same tropical average time series used in Dessler et al. (2013, 2014): ΔT is tropical averaged tropospheric temperature anomaly at 500 hPa, with units of degrees K. BDC is a Brewer-Dobson circulation index — here we use the tropical averaged diabatic heating rate anomaly at 82-hPa as a surrogate, with units of $\mathrm{K\ day^{-1}}$. QBO is a quasi-biennial oscillation index and here we use standardized monthly and zonally averaged equatorial zonal winds anomaly at 50-hPa. Because these regressors are tropical average values, they do not vary with location. The QBO index is lagged by 2 months in the regression because the phase of the QBO takes time to impact TTL temperature and then the water vapor at 100 hPa (Dessler et al., 2013). There is no lag for the BDC and ΔT indices in this study.

Atmos. Chem. Phys. Discuss., https://doi.org/10.5194/acp-2017-951
Manuscript under review for journal Atmos. Chem. Phys.
Discussion started: 25 October 2017

Atmospheric Chemistry and Physics Discussions

We first analyze MLS H_2O observations. We run the regression on these observations twice: once using BDC and ΔT regressors from the ERAi reanalysis and again using regressors from the MERRA-2 reanalysis. The QBO index is the same in both regressions (we use NCEP observations downloaded from http://www.cpc.ncep.noaa.gov/data/indices/qbo.u50.index).

The BDC coefficients (Figs. 2a and 2d) are negative over the tropics, consistent with the idea that an enhanced Brewer-Dobson Circulation cools the TTL (Yulaeva et al., 1994; Randel et al., 2006) and reduces water vapor (Dhomse et al., 2008). The QBO coefficients (Figs. 3a and 3d) are positive over almost all of the tropics, as the positive phase of QBO tends to decrease the upwelling in TTL, thereby warming it (Plumb and Bell, 1982; Davis et al., 2013).

We also run the regression on H_2O simulated by the trajectory model. We use BDC and ΔT regressors from the same reanalysis used to drive each trajectory model (i.e., we use ERAi regressors to analyze the ERAi-driven trajectory model); the QBO index is always from the NCEP observations.

The BDC coefficients from regression of the trajectory models (Figs. 2b and 2e) agree well with the coefficients from the regressions of the MLS observations. The gridpoint-by-gridpoint scatter plots (MLS vs. trajectory; Figs. 2c and 2f) demonstrate this agreement in more detail. The only clear difference is that the regression of the MLS data using MERRA-2 regressors produces BDC coefficients that tend to be more negative than those from the trajectory model driven by MERRA-2 meteorology.

The QBO coefficients from the regressions of the trajectory models are shown in Figs. 3b and 3e with gridpoint-by-gridpoint scatter plots in Figs. 3c and 3f. As with the BDC comparison, the trajectory models do a good job reproducing the regressions of the MLS data.

Dotted regions in Figs 2 and 3 indicate where the coefficients are statistically different from zero at a 95% significance level with a *t*-test. When testing the significance of coefficients, the autocorrelation in the time series is accounted for following Santer et al. (2000) by reducing the number of degrees of freedom from the lag-1 autocorrelation of the residual time series.

Overall, we conclude that the trajectory model accurately captures the impact of the BDC and QBO on TTL water vapor — for both the tropical average and the spatial distribution. This supports the hypothesis that these processes mainly influence TTL water vapor by varying large-scale TTL temperatures (Giorgetta and Bengtsson, 1999; Randel et al., 2000; Geller et al., 2002; Randel et al., 2006; Dhomse et al., 2008; Liang et al., 2011; Davis et al., 2013; Dessler et al., 2013; Wang et al., 2015), which we expect the trajectory model to reproduce well.

3.2 Influence of tropospheric temperature (ΔT) on TTL water

Coefficients of ΔT from the MLS regressions are mostly positive, with large increases over the Tropical Warm Pool region (TWP) and Indian Ocean (Figs. 4a and 4e), indicating that warming of the tropical troposphere increases the 100 hPa water vapor mixing ratio there. Over the Central Equatorial Pacific (CEP), however, a warming troposphere decreases water vapor.

The decrease in water vapor in the CEP is not entirely unexpected. TTL temperatures are usually coldest — and water vapor a minimum — above the convection maximum in the TWP. As ΔT increases in response to an El Niño event, convection shifts from the TWP to the CEP. As this occurs, the cold pool moves to the CEP, so the CEP cools and the TWP warms (Davis et al., 2013; Hu et al., 2016; Avery et al., 2017). Changes in TTL H_2O are expected to mirror this, with increases in water vapor in

Atmos. Chem. Phys. Discuss., https://doi.org/10.5194/acp-2017-951
Manuscript under review for journal Atmos. Chem. Phys.
Discussion started: 25 October 2017

Atmospheric Chemistry and Physics Discussions

the TWP and decreases in the CEP as ΔT increases. The trajectory models, in which temperature is the only regulator, clearly show this dipole pattern (Figs. 4b and 4e).

The fits to the MLS data (Figs. 4a and 4d) show ΔT coefficients in the TWP similar to those seen in the trajectory models. In the CEP, however, both MLS regressions show less negative coefficients than those found in the trajectory regressions (Figs. 4c and 4f).

We hypothesize that the evaporation of convective ice accounts for the difference between the ΔT coefficients in the MLS and trajectory-model regressions. As convection moves eastward during an El Niño event, there is an increase in ice injected into the TTL in the CEP (Avery et al., 2017), where it evaporates and hydrates the TTL (Ueyama et al., 2015; Schoeberl et al., 2014). This evaporation partially offsets reductions in H_2O due to local cooling of the TTL. As a result, the net decrease in H_2O in the CEP in response to changes in ΔT is smaller in the observations than in the trajectory model, which only includes the changes in TTL temperature.

Support for this hypothesis can be found in Figs. 5a and 5b, which shows the temperature anomalies at 100 hPa (T_{100}) in the two ENSO phases. The T_{100} anomalies clearly show the zonal shift of negative anomalies from the TWP during La Niña to the CEP during El Niño. The figure also shows observed cloud occurrence anomaly above the 365-K potential temperature level during El Niño and La Niña phases. These data show that the deep convective clouds shift from the TWP eastward to the CEP as well. This confirms CALIPSO observations of increased ice in the CEP during the exceptional El Niño event in 2015-2016 (Avery et al., 2017).

Thus, observations of convective clouds are consistent with the hypothesis that evaporation of ice in the CEP during El Niño events adds water vapor that mostly cancels the influence of the decrease in temperature of the region.

3.3 Tests with a climate model

To more quantitatively test our hypothesis that evaporation of convective ice plays a role in the TTL water budget, we perform a parallel analysis with the GEOSCCM. We run the regression on the GEOSCCM 100 hPa H_2O fields as well as on H_2O simulated by a trajectory model driven by the GEOSCCM meteorology. Dessler et al. (2016) demonstrated the utility of this comparison in showing that convective ice evaporation plays an important role in the long-term trend in stratospheric water in this model.

Figs. 2g and 2h show the spatial distribution of the BDC coefficients from the GEOSCCM and the corresponding trajectory model. The coefficients are similar to each other and similar to the MLS regressions, suggesting that the GEOSCCM is accurately simulating the impact of BDC changes on TTL water vapor. The version of the GEOSCCM analyzed here does not include a QBO, so there is no GEOSCCM QBO coefficient in Fig. 3.

Before we discuss the ΔT coefficients, it is worth pointing out that the GEOSCCM has realistic interannual variability in T_{100} and convective ice. Figs. 5c and 5d show the monthly convective cloud ice water content (IWC) anomalies at 118 hPa from GEOSCCM during ENSO-like warm and cold phases, respectively. It shows positive convective ice anomalies shift eastward as the ΔT warms from a cold phase (Fig. 5d) to a warm phase (Fig. 5c), with a similar zonal shift in temperature anomalies at 100 hPa. These compare well with the observations (Fig. 5a and 5b).

Atmos. Chem. Phys. Discuss., https://doi.org/10.5194/acp-2017-951
Manuscript under review for journal Atmos. Chem. Phys.
Discussion started: 25 October 2017

Atmospheric Chemistry and Physics Discussions

The ΔT coefficient fields from the GEOSCCM and associated trajectory regressions (Fig. 4g and 4h) show the same structural differences as do the ΔT coefficients from the MLS and accompanying trajectory model regressions — that the ΔT coefficient in the CEP is less negative in the GEOSCCM regression than in the trajectory regression. Since previous analysis of the GEOSCCM demonstrated that evaporation of convective ice from convection increases TTL water vapor (Dessler et al., 2016), it may be possible to demonstrate that evaporation of convective ice is responsible for this difference.

To directly test this hypothesis, we run a second version of the traj_ccm model that includes the evaporation of convective ice from GEOSCCM, referred to hereafter as traj_ccm_ice. In this trajectory model run, we use the 6-hourly three-dimensional convective cloud IWC fields from GEOSCCM and linearly interpolate it to each parcel's position at every time step. We then assume instantaneous and complete evaporation of this ice into the parcel by adding the IWC to the parcel's water vapor, although we do not let parcels exceed 100% relative humidity with respect to ice. This is the same procedure used to simulate convective ice evaporation by Dessler et al. (2016) .

We then run the regression on the traj_ccm_ice's H_2O field with the BDC and ΔT terms from GEOSCCM. The BDC coefficients change little in the CEP (Fig. 2j) when including the evaporation of convective ice. The point-by-point scatter plot in Fig. 2k shows more scatter after we add ice evaporation, a likely result of the crudeness of our instant evaporation assumption. That said, the addition of evaporation of convective ice to the model eliminates most of the negative coefficients in the CEP and brings the trajectory model into closer agreement with the GEOSCCM (seen by comparing Figs 4g to 4j).

To better understand this result, we calculate the evaporation rate of convective ice at 100 hPa in the trajectory model. To do this, we save the amount of water added to each parcel by ice evaporation in every time step. We then bin and average the amount evaporated to come up with the distribution of the amount evaporated per day between 109 and 93 hPa. Fig. 6 shows the distribution of monthly averaged evaporation rate anomalies during the ENSO-like warm and cold phases in the GEOSCCM.

We see that, as ΔT increases and we transit from a cold to a warm phase, the TTL convective cloud evaporation rate increases in the CEP and Latin America areas and decreases in the TWP and Indian Ocean areas. This confirms that ice evaporation increases TTL water vapor in the CEP and cancels out the drying effect of decreasing temperatures there in the GEOSCCM.

To conclude, our hypothesis that evaporation of convective ice moistens the TTL in the CEP is supported qualitatively by observations showing that clouds in the CEP increase with ΔT (Fig. 5; also Avery et al., 2017). It is also supported quantitatively by the GEOSCCM, which shows variations of TTL water vapor similar to the observations and that convective ice plays a key role in those variations. Given how accurately the GEOSCCM simulates water vapor in the TTL, we view this as support for our hypothesis.

Our work should not be taken as opposing previous work (Randel et al., 2006; Schiller et al., 2009; Wright et al., 2011; Randel and Jensen, 2013; Dessler et al., 2016) that concludes most of the variance in TTL water vapor over the last few decades is due to TTL temperature. We concur that the impact of convective ice only is a relatively minor contributor to TTL water vapor variability over the period spanned by the MLS data. But the GEOSCCM, which does an excellent job simulating TTL water vapor over this period, suggests that convective ice may play an important role in long-term trends of stratospheric water vapor (Dessler et al., 2016).

Atmos. Chem. Phys. Discuss., https://doi.org/10.5194/acp-2017-951
Manuscript under review for journal Atmos. Chem. Phys.
Discussion started: 25 October 2017

Atmospheric Chemistry and Physics Discussions

4 Conclusions

Previous work has shown that tropical average TTL water vapor variations can be attributed to physical processes correlated with three regressors: the tropical tropospheric temperature (ΔT), the Brewer-Dobson circulation (BDC), and the quasi-biennial oscillation (QBO) (Dessler et al., 2013, 2014). We extend these previous analyses and focus on the physical processes controlling the spatial distribution of TTL water vapor.

To do that, we use a linear regression on TTL water vapor at individual grid points over the tropics to investigate the spatial distribution of the impact of the BDC, QBO, and ΔT indices. The spatial pattern and magnitude of the BDC and QBO coefficients agree well between MLS observations and associated trajectory model simulations. This suggests that, consistent with expectations, these processes affect TTL water vapor mainly by changing TTL temperatures (Randel et al., 2000; Geller et al., 2002; Randel et al., 2006; Dhomse et al., 2008; Liang et al., 2011; Dessler et al., 2013; Davis et al., 2013). The GEOSCCM also produces similar coefficient fields, building confidence in that model's ability to simulate TTL water.

The spatial distribution of ΔT coefficients has an obvious dipole structure with negative values in the Central Equatorial Pacific (CEP), where temperatures decrease as the troposphere warms, and positive values in the Tropical Warm Pool (TWP), where the opposite occurs. The trajectory model analyses produce more negative values in the CEP, consistent with the strong cooling there as the troposphere warms. The MLS analysis, however, does not do this.

We hypothesized that an increase of deep convection as the troposphere warms increases evaporation of convective ice in the CEP. This ice evaporates, offsetting the reduction in water vapor there due to the decreasing temperatures. We see evidence of increases in convective clouds reaching the TTL in the CEP as ΔT increases in observations, in agreement with previous work (Avery et al., 2017). Tests of the GEOSCCM model show that this process is occurring in that model.

Thus, we conclude that evaporation of convective ice likely plays a role in setting the distribution of water vapor in the TTL. However, this effect is minor on interannual time scales; most of the variance is due to other processes that change TTL temperatures. However, it may play a much larger role in long-term trends of TTL and stratospheric water vapor (Dessler et al., 2016).

Competing interests. We have no competing interests.

Acknowledgements. We thank Mark Schoeberl for his insights into this problem. This work was supported by NASA grant NNX14AF15G to Texas A&M University.

Atmos. Chem. Phys. Discuss., https://doi.org/10.5194/acp-2017-951
Manuscript under review for journal Atmos. Chem. Phys.
Discussion started: 25 October 2017

Atmospheric Chemistry and Physics Discussions

References

Anderson, J. G., Wilmouth, D. M., Smith, J. B., Sayres, D. S., et al.: UV dosage levels in summer: Increased risk of ozone loss from convectively injected water vapor, Science, 337, 835–839, 2012.

Avery, M. A., Davis, S. M., Rosenlof, K. H., Ye, H., and Dessler, A. E.: Large anomalies in lower stratospheric water vapour and ice during the 2015-2016 El Niño, Nature Geoscience, 10, 405–409, 2017.

Barahona, D., Molod, A., Bacmeister, J., Nenes, A., Gettelman, A., Morrison, H., Phillips, V., and Eichmann, A.: Development of two-moment cloud microphysics for liquid and ice within the NASA Goddard Earth Observing System Model (GEOS-5), Geoscientific Model Development, 7, 1733–1766, 2014.

Bergman, J. W., Jensen, E. J., Pfister, L., and Yang, Q.: Seasonal differences of vertical-transport efficiency in the tropical tropopause layer: On the interplay between tropical deep convection, large-scale vertical ascent, and horizontal circulations, Journal of Geophysical Research: Atmospheres, 117, 2012.

Bosilovich, M., Lucchesi, R., and Suarez, M.: MERRA-2: File specification, GMAO Office Note No. 9 (Version 1.1), Tech. Rep. Version 1.1, Global Modeling and Assimilation Office, 2016.

Bowman, K. P.: Large-scale isentropic mixing properties of the Antarctic polar vortex from analyzed winds, Journal of Geophysical Research: Atmospheres, 98, 23 013–23 027, 1993.

Bowman, K. P. and Carrie, G. D.: The mean-meridional transport circulation of the troposphere in an idealized GCM, Journal of the Atmospheric Sciences, 59, 1502–1514, 2002.

Calvo, N., Garcia, R., Randel, W., and Marsh, D.: Dynamical mechanism for the increase in tropical upwelling in the lowermost tropical stratosphere during warm ENSO events, Journal of the Atmospheric Sciences, 67, 2331–2340, 2010.

Carminati, F., Ricaud, P., Pommereau, J.-P., Rivière, E., Khaykin, S., Attié, J.-L., and Warner, J.: Impact of tropical land convection on the water vapour budget in the tropical tropopause layer, Atmospheric Chemistry and Physics, 14, 6195–6211, 2014.

Corti, T., Luo, B., De Reus, M., Brunner, D., Cairo, F., Mahoney, M., Martucci, G., Matthey, R., Mitev, V., Dos Santos, F., et al.: Unprecedented evidence for deep convection hydrating the tropical stratosphere, Geophysical Research Letters, 35, 2008.

Davis, S. M., Liang, C. K., and Rosenlof, K. H.: Interannual variability of tropical tropopause layer clouds, Geophysical Research Letters, 40, 2862–2866, 2013.

Dee, D., Uppala, S., Simmons, A., Berrisford, P., Poli, P., Kobayashi, S., Andrae, U., Balmaseda, M., Balsamo, G., Bauer, P., et al.: The ERA-Interim reanalysis: Configuration and performance of the data assimilation system, Quarterly Journal of the Royal Meteorological Society, 137, 553–597, 2011.

Dessler, A. and Sherwood, S.: Effect of convection on the summertime extratropical lower stratosphere, Journal of Geophysical Research: Atmospheres, 109, 2004.

Dessler, A., Hanisco, T., and Fueglistaler, S.: Effects of convective ice lofting on H_2O and HDO in the tropical tropopause layer, Journal of Geophysical Research: Atmospheres, 112, 2007.

Dessler, A., Schoeberl, M., Wang, T., Davis, S., and Rosenlof, K.: Stratospheric water vapor feedback, Proceedings of the National Academy of Sciences, 110, 18 087–18 091, 2013.

Dessler, A., Schoeberl, M., Wang, T., Davis, S., Rosenlof, K., and Vernier, J.-P.: Variations of stratospheric water vapor over the past three decades, Journal of Geophysical Research: Atmospheres, 119, 2014.

Dessler, A., Ye, H., Wang, T., Schoeberl, M., Oman, L., Douglass, A., Butler, A., Rosenlof, K., Davis, S., and Portmann, R.: Transport of ice into the stratosphere and the humidification of the stratosphere over the 21st century, Geophysical Research Letters, 2016.

Dhomse, S., Weber, M., and Burrows, J.: The relationship between tropospheric wave forcing and tropical lower stratospheric water vapor, Atmospheric Chemistry and Physics, 8, 471–480, 2008.

Duncan, B., Strahan, S., Yoshida, Y., Steenrod, S., and Livesey, N.: Model study of the cross-tropopause transport of biomass burning pollution, Atmospheric Chemistry and Physics, 7, 3713–3736, 2007.

Frey, W., Schofield, R., Hoor, P., Kunkel, D., Ravegnani, F., Ulanovsky, A., Viciani, S., D'amato, F., and Lane, T.: The impact of overshooting deep convection on local transport and mixing in the tropical upper troposphere/lower stratosphere (UTLS), Atmospheric Chemistry and Physics, 15, 6467–6486, 2015.

Fueglistaler, S. and Haynes, P.: Control of interannual and longer-term variability of stratospheric water vapor, Journal of Geophysical Research: Atmospheres, 110, 2005.

Fueglistaler, S., Dessler, A., Dunkerton, T., Folkins, I., Fu, Q., and Mote, P. W.: Tropical tropopause layer, Reviews of Geophysics, 47, 2009.

Geller, M. A., Zhou, X., and Zhang, M.: Simulations of the interannual variability of stratospheric water vapor, Journal of the Atmospheric Sciences, 59, 1076–1085, 2002.

Gettelman, A., Liu, X., Ghan, S. J., Morrison, H., Park, S., Conley, A., Klein, S. A., Boyle, J., Mitchell, D., and Li, J.-L.: Global simulations of ice nucleation and ice supersaturation with an improved cloud scheme in the Community Atmosphere Model, Journal of Geophysical Research: Atmospheres, 115, 2010.

Giorgetta, M. A. and Bengtsson, L.: Potential role of the quasi-biennial oscillation in the stratosphere-troposphere exchange as found in water vapor in general circulation model experiments, Journal of Geophysical Research: Atmospheres, 104, 6003–6019, 1999.

Hassim, M. and Lane, T.: A model study on the influence of overshooting convection on TTL water vapour, Atmospheric Chemistry and Physics, 10, 9833–9849, 2010.

Herman, R. L., Ray, E. A., Rosenlof, K. H., Bedka, K. M., Schwartz, M. J., Read, W. G., Troy, R. F., Chin, K., Christensen, L. E., Fu, D., Stachnik, R. A., Bui, T. P., and Dean-Day, J. M.: Enhanced stratospheric water vapor over the summertime continental United States and the role of overshooting convection, Atmospheric Chemistry and Physics, 17, 6113, 2017.

Holton, J. R. and Gettelman, A.: Horizontal transport and the dehydration of the stratosphere, Geophysical Research Letters, 28, 2799–2802, 2001.

Hu, D., Tian, W., Guan, Z., Guo, Y., and Dhomse, S.: Longitudinal asymmetric trends of tropical cold-point tropopause temperature and their link to strengthened walker circulation, Journal of Climate, 29, 7755–7771, 2016.

Khaykin, S., Pommereau, J.-P., Korshunov, L., Yushkov, V., Nielsen, J., Larsen, N., Christensen, T., Garnier, A., Lukyanov, A., and Williams, E.: Hydration of the lower stratosphere by ice crystal geysers over land convective systems, Atmospheric Chemistry and Physics, 9, 2275–2287, 2009.

Lambert, A., Read, W., Livesey, N., Santee, M., Manney, G., Froidevaux, L., Wu, D., Schwartz, M., Pumphrey, H., Jimenez, C., et al.: Validation of the Aura Microwave Limb Sounder middle atmosphere water vapor and nitrous oxide measurements, Journal of Geophysical Research: Atmospheres, 112, 2007.

Liang, C., Eldering, A., Gettelman, A., Tian, B., Wong, S., Fetzer, E., and Liou, K.: Record of tropical interannual variability of temperature and water vapor from a combined AIRS-MLS data set, Journal of Geophysical Research: Atmospheres, 116, 2011.

Livesey, N. J., Read, W. G., Wagner, P. A., Froidevaux, L., Lambert, A., Manney, G. L., Millán-Valle, L. F., Pumphrey, H. C., Santee, M. L., Schwartz, M. J., Wang, S., Fuller, R. A., Jarnot, R. F., Knosp, B. W., and Martinez, E.: Earth Observing System (EOS) Aura Microwave

Limb Sounder (MLS), Version 4.2x Level 2 data quality and description document, Tech. Rep. JPL D-33509, Tech. Rep. version 4.2x-3.0, NASA Jet Propulsion Laboratory, 2017.

Molod, A., Takacs, L., Suarez, M., Bacmeister, J., Song, I.-S., and Eichmann, A.: The GEOS-5 atmospheric general circulation model: Mean climate and development from MERRA to Fortuna, Technical Report Series on Global Modeling and Data Assimilation Volume 28, NASA Goddard Space Flight Center, 2012.

Mote, P. W., Rosenlof, K. H., McIntyre, M. E., Carr, E. S., Gille, J. C., Holton, J. R., Kinnersley, J. S., Pumphrey, H. C., Russell, J. M., and Waters, J. W.: An atmospheric tape recorder: The imprint of tropical tropopause temperatures on stratospheric water vapor, Journal of Geophysical Research: Atmospheres, 101, 3989–4006, 1996.

Murphy, D. and Koop, T.: Review of the vapour pressures of ice and supercooled water for atmospheric applications, Quarterly Journal of the Royal Meteorological Society, 131, 1539–1565, 2005.

Pfister, L., Selkirk, H. B., Jensen, E. J., Schoeberl, M. R., Toon, O. B., Browell, E. V., Grant, W. B., Gary, B., Mahoney, M. J., Bui, T. V., and Hintsa, E.: Aircraft observations of thin cirrus clouds near the tropical tropopause, Journal of Geophysical Research: Atmospheres, 106, 9765–9786, 2001.

Plumb, R. A. and Bell, R. C.: A model of the quasi-biennial oscillation on an equatorial beta-plane, Quarterly Journal of the Royal Meteorological Society, 108, 335–352, 1982.

Randel, W. J. and Jensen, E. J.: Physical processes in the tropical tropopause layer and their roles in a changing climate, Nature Geoscience, 6, 169–176, 2013.

Randel, W. J., Wu, F., and Gaffen, D. J.: Interannual variability of the tropical tropopause derived from radiosonde data and NCEP reanalyses, Journal of Geophysical Research: Atmospheres, 105, 15–509, 2000.

Randel, W. J., Wu, F., Voemel, H., Nedoluha, G. E., and Forster, P.: Decreases in stratospheric water vapor after 2001: Links to changes in the tropical tropopause and the Brewer-Dobson circulation, Journal of Geophysical Research: Atmospheres, 111, 2006.

Read, W., Lambert, A., Bacmeister, J., Cofield, R., Christensen, L., Cuddy, D., Daffer, W., Drouin, B., Fetzer, E., Froidevaux, L., et al.: Aura Microwave Limb Sounder upper tropospheric and lower stratospheric H_2O and relative humidity with respect to ice validation, Journal of Geophysical Research: Atmospheres, 112, 2007.

Santer, B. D., Wigley, T., Boyle, J., Gaffen, D. J., Hnilo, J., Nychka, D., Parker, D., and Taylor, K.: Statistical significance of trends and trend differences in layer-average atmospheric temperature time series, Journal of Geophysical Research: Atmospheres, 105, 7337–7356, 2000.

Schiller, C., Grooß, J.-U., Konopka, P., Plöger, F., Silva dos Santos, F., and Spelten, N.: Hydration and dehydration at the tropical tropopause, Atmospheric Chemistry and Physics, 9, 9647–9660, 2009.

Schoeberl, M. and Dessler, A.: Dehydration of the stratosphere, Atmospheric Chemistry and Physics, 11, 8433–8446, 2011.

Schoeberl, M., Dessler, A., and Wang, T.: Simulation of stratospheric water vapor and trends using three reanalyses, Atmospheric Chemistry and Physics, 12, 6475–6487, 2012.

Schoeberl, M., Dessler, A., and Wang, T.: Modeling upper tropospheric and lower stratospheric water vapor anomalies, Atmospheric Chemistry and Physics, 13, 7783–7793, 2013.

Schoeberl, M. R., Dessler, A. E., Wang, T., Avery, M. A., and Jensen, E. J.: Cloud formation, convection, and stratospheric dehydration, Earth and Space Science, 1, 1–17, 2014.

Schwartz, M. J., Read, W. G., Santee, M. L., Livesey, N. J., Froidevaux, L., Lambert, A., and Manney, G. L.: Convectively injected water vapor in the North American summer lowermost stratosphere, Geophysical Research Letters, 40, 2316–2321, 2013.

Sherwood, S. C. and Dessler, A. E.: On the control of stratospheric humidity, Geophysical Research Letters, 27, 2513–2516, 2000.

Solomon, S., Rosenlof, K. H., Portmann, R. W., Daniel, J. S., Davis, S. M., Sanford, T. J., and Plattner, G.-K.: Contributions of stratospheric water vapor to decadal changes in the rate of global warming, Science, 327, 1219–1223, 2010.

Stenke, A. and Grewe, V.: Simulation of stratospheric water vapor trends: impact on stratospheric ozone chemistry, Atmospheric Chemistry and Physics, 5, 1257–1272, 2005.

Sun, Y. and Huang, Y.: An examination of convective moistening of the lower stratosphere using satellite data, Earth and Space Science, 2, 320–330, 2015.

Ueyama, R., Jensen, E. J., Pfister, L., and Kim, J.-E.: Dynamical, convective, and microphysical control on wintertime distributions of water vapor and clouds in the tropical tropopause layer, Journal of Geophysical Research: Atmospheres, 120, 2015.

Virts, K. S. and Houze Jr, R. A.: Clouds and water vapor in the tropical tropopause transition layer over mesoscale convective systems, Journal of the Atmospheric Sciences, 72, 4739–4753, 2015.

Wang, T., Randel, W., Dessler, A., Schoeberl, M., and Kinnison, D.: Trajectory model simulations of ozone (O_3) and carbon monoxide (CO) in the lower stratosphere, Atmospheric Chemistry and Physics, 14, 7135–7147, 2014.

Wang, W., Matthes, K., and Schmidt, T.: Quantifying contributions to the recent temperature variability in the tropical tropopause layer, Atmospheric Chemistry and Physics, 15, 5815–5826, 2015.

Wright, J., Fu, R., Fueglistaler, S., Liu, Y., and Zhang, Y.: The influence of summertime convection over Southeast Asia on water vapor in the tropical stratosphere, Journal of Geophysical Research: Atmospheres, 116, 2011.

Wright, J. S., Sobel, A. H., and Schmidt, G. A.: Influence of condensate evaporation on water vapor and its stable isotopes in a GCM, Geophysical Research Letters, 36, 2009.

Yulaeva, E., Holton, J. R., and Wallace, J. M.: On the cause of the annual cycle in tropical lower-stratospheric temperatures, Journal of the Atmosperic Sciences, 51, 169–174, 1994.

Atmos. Chem. Phys. Discuss., https://doi.org/10.5194/acp-2017-951
Manuscript under review for journal Atmos. Chem. Phys.
Discussion started: 25 October 2017

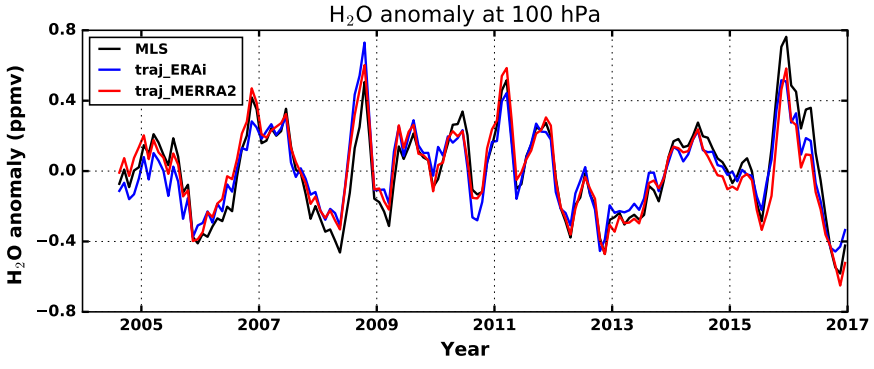

Figure 1. Tropical (30°N-30°S) monthly water vapor anomalies at 100 hPa from MLS observations (black line) and from trajectory model runs driven by ERAi (blue line) and MERRA-2 (red line) from August 2004 through 2016. Anomalies are calculated by subtracting the mean annual cycle from the observations.

Atmos. Chem. Phys. Discuss., https://doi.org/10.5194/acp-2017-951
Manuscript under review for journal Atmos. Chem. Phys.
Discussion started: 25 October 2017

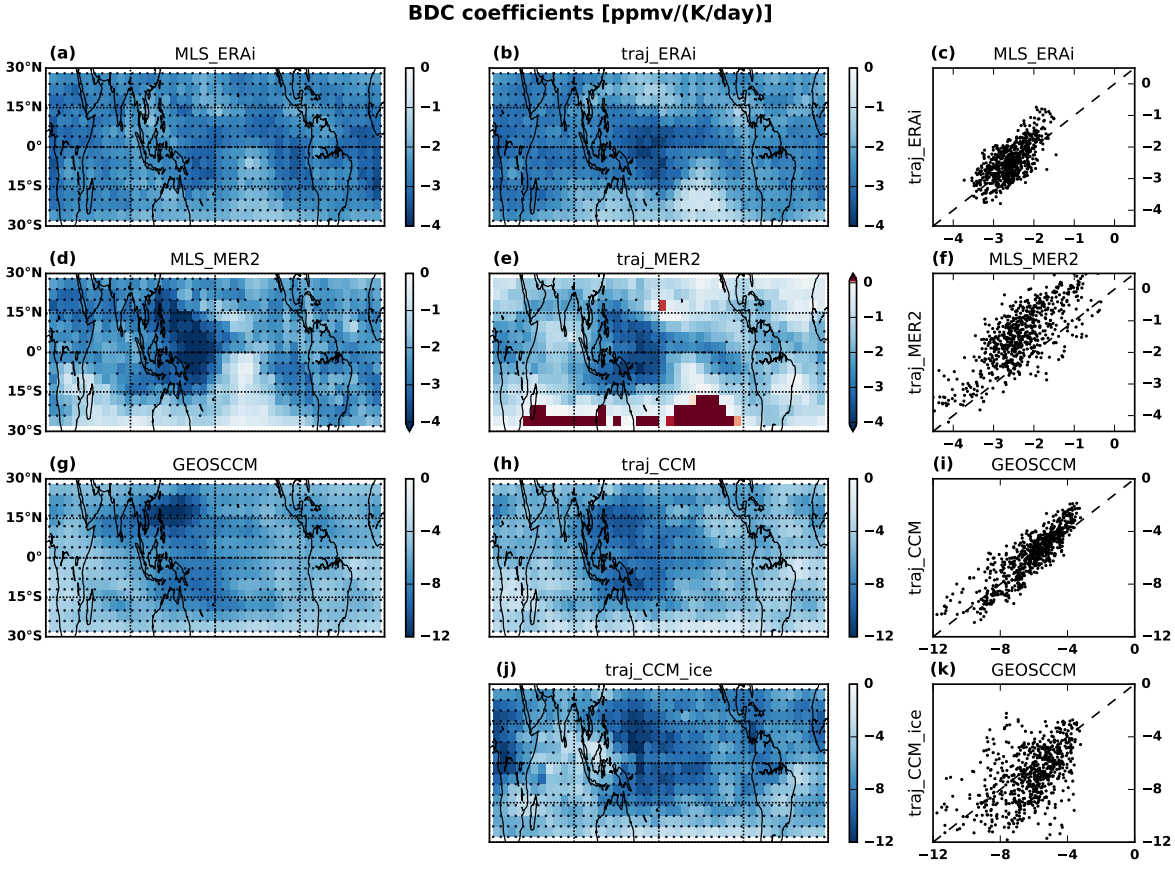

Figure 2. Multivariate linear regression coefficients of the BDC regressor from MLS and GEOSCCM H_2O fields (left column), as well as the coefficients from regression of the associated trajectory model fields (middle column). Scatter plots of MLS/GEOSCCM regressions vs. trajectory model regressions indicate the similarity of the fields (right column). The MLS and associated trajectory regressions cover the period August 2004 to December 2016 between 30°N and 30°S. The GEOSCCM and associated trajectory run cover 2005-2016 model years. The bottom row shows coefficients from regressions of a run of the trajectory model driven by GEOSCCM meteorology that includes evaporation of convective ice. The black dots in the first two columns indicate where coefficients are non-zero with a significance level of 95%.

Atmos. Chem. Phys. Discuss., https://doi.org/10.5194/acp-2017-951
Manuscript under review for journal Atmos. Chem. Phys.
Discussion started: 25 October 2017

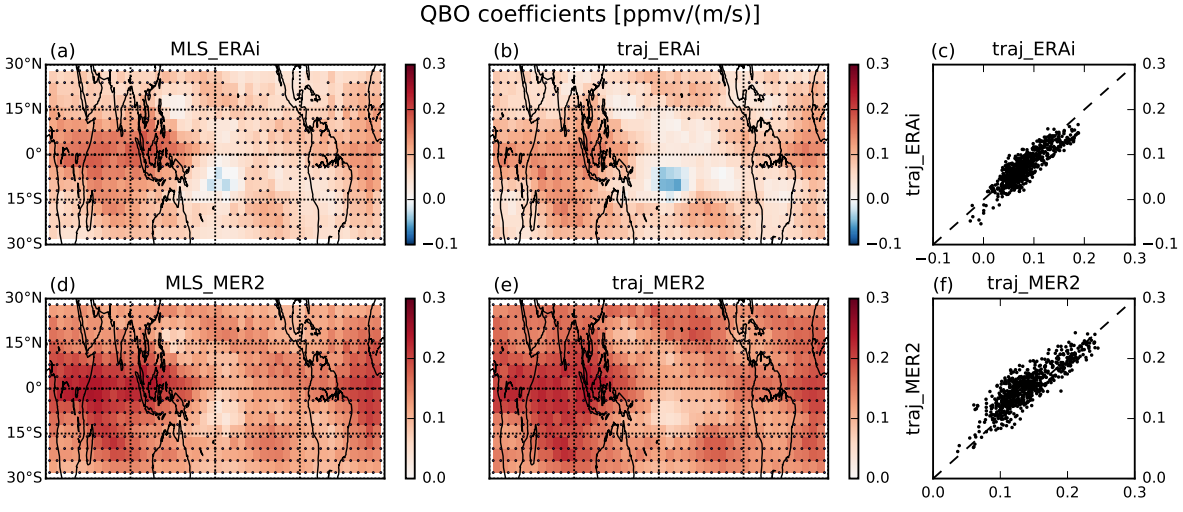

Figure 3. Same as Fig. 2, but for coefficients of the QBO regressor. This GEOSCCM run does not simulate a QBO, so it has been omitted.

Atmos. Chem. Phys. Discuss., https://doi.org/10.5194/acp-2017-951
Manuscript under review for journal Atmos. Chem. Phys.
Discussion started: 25 October 2017

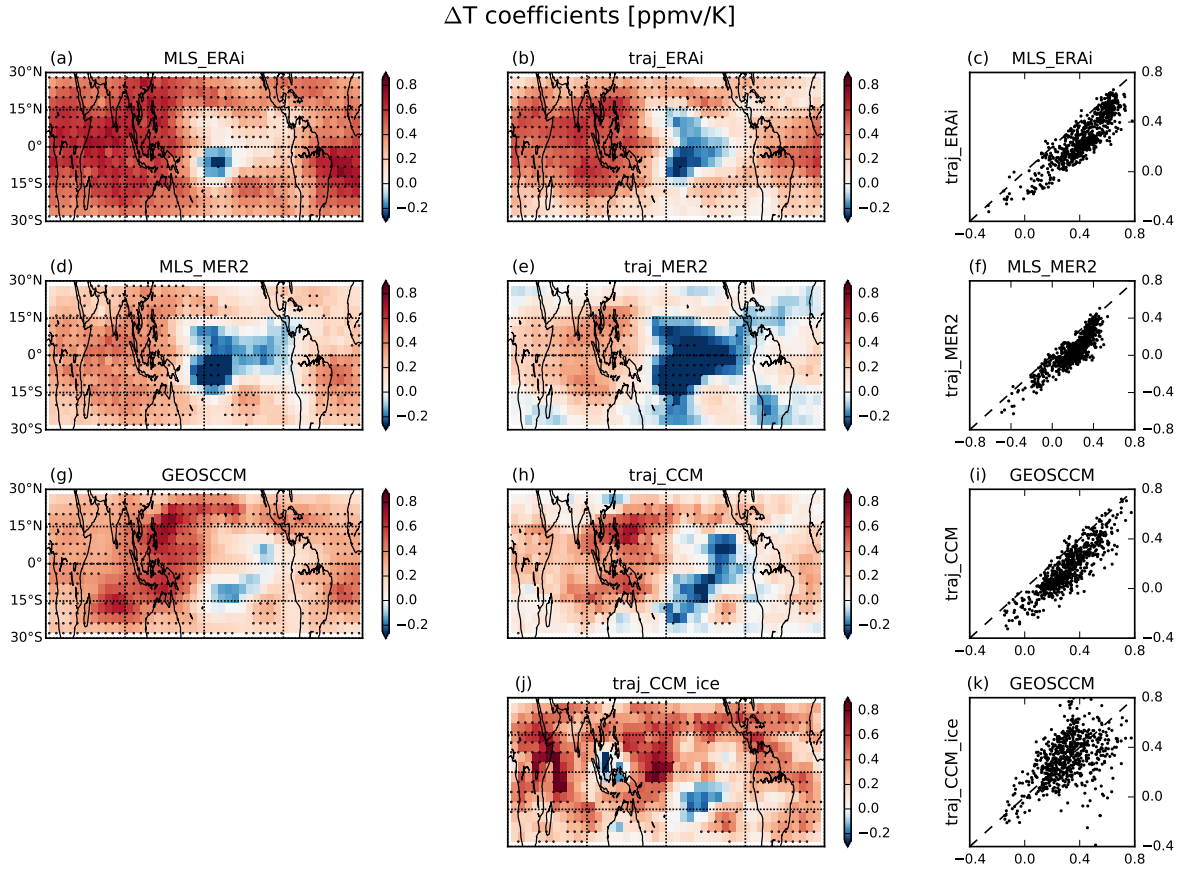

Figure 4. Same as Fig. 2 but for the coefficient of the ΔT regressor.

Atmos. Chem. Phys. Discuss., https://doi.org/10.5194/acp-2017-951
Manuscript under review for journal Atmos. Chem. Phys.
Discussion started: 25 October 2017

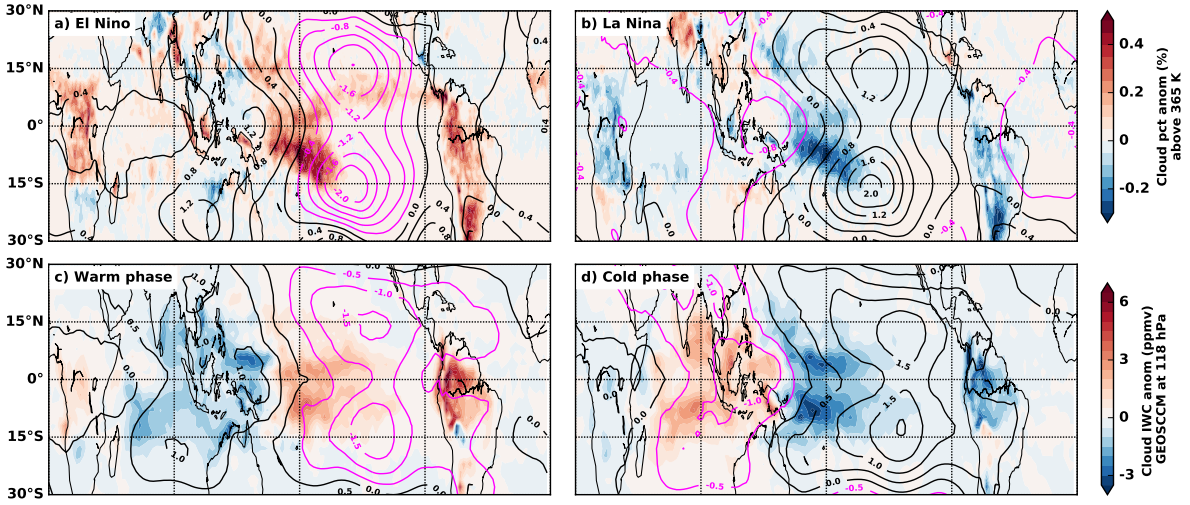

Figure 5. Averaged monthly cloud occurrence anomalies above 365 K during (a) El Niño and (b) La Niña months from 2005 to 2016 with averaged ERAi temperature anomalies at 100 hPa shown as contours. El Niño and La Niña months are based on the NOAA Oceanic Niño Index (ONI) in the Niño 3.4 region (5°S to 5°N; 170°W to 120°W). Averaged monthly GEOSCCM convective cloud ice water content (IWC) anomalies (ppmv) at 118 hPa during (c) warm and (d) cold GEOSCCM phases from model years 2005 to 2016 with averaged temperature anomalies at 100 hPa shown as contours. The warm and cold phases are defined to be GEOSCCM surface temperature anomaly (departures from the mean annual cycle) of +0.5 K and -0.5 K, respectively, in the Niño 3.4 region (same as ONI). In all panels, magenta and black contours show positive and negative temperature anomalies, respectively.

Atmos. Chem. Phys. Discuss., https://doi.org/10.5194/acp-2017-951
Manuscript under review for journal Atmos. Chem. Phys.
Discussion started: 25 October 2017

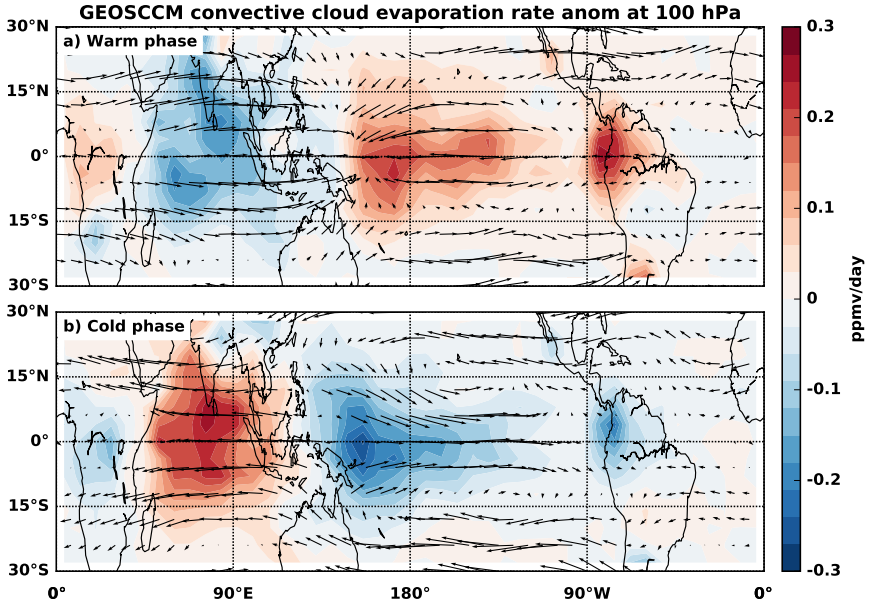

Figure 6. Averaged monthly GEOSCCM convective cloud evaporation rate anomalies at 100 hPa during (a) warm and (b) cold GEOSCCM phases from 2005 to 2016. Also shown are averaged horizontal wind anomaly vectors at 100 hPa.